

# Magnetic Field-Induced Condensation of Triplons in Han Purple Pigment $\text{BaCuSi}_2\text{O}_6$

M. Jaime<sup>1\*</sup>, V. F. Correa<sup>1</sup>, N. Harrison<sup>1</sup>, C. D. Batista<sup>2</sup>, N. Kawashima<sup>3</sup>, Y. Kazuma<sup>3</sup>, G.  
A. Jorge<sup>1,4</sup>, R. Stern<sup>5</sup>, I. Heinmaa<sup>5</sup>, S. A. Zvyagin<sup>6</sup>, Y. Sasago<sup>7†</sup>, K. Uchinokura<sup>7††</sup>

<sup>1</sup> *National High Magnetic Field Laboratory,  
MS-E536, Los Alamos, NM 87545, USA.*

<sup>2</sup> *Theoretical Division, Los Alamos, NM 87545, USA.*

<sup>3</sup> *Department of Physics, Tokyo Metropolitan University, Tokyo 192-0397, Japan.*

<sup>4</sup> *Departamento de Física, Universidad de Buenos Aires, Argentina.*

<sup>5</sup> *National Institute of Chemical Physics and Biophysics, 12618 Tallinn, Estonia.*

<sup>6</sup> *National Magnetic Field Laboratory, Tallahassee, FL 32310, USA. and*

<sup>7</sup> *Department of Applied Physics, The University of Tokyo, Tokyo, 113-8656, Japan.*

## Abstract

Besides being an ancient pigment,  $\text{BaCuSi}_2\text{O}_6$  is a quasi-2D magnetic insulator with a gapped spin dimer ground state. The application of strong magnetic fields closes this gap creating a gas of bosonic spin triplet excitations called triplons. The topology of the spin lattice makes  $\text{BaCuSi}_2\text{O}_6$  an ideal candidate for studying the Bose-Einstein condensation of triplons as a function of the external magnetic field, which acts as a chemical potential. In agreement with quantum Monte Carlo numerical simulation, we observe a distinct lambda-anomaly in the specific heat together with a maximum in the magnetic susceptibility upon cooling down to liquid Helium temperatures.

PACS numbers: 75.45.+j, 75.40.Cx, 05.30.Jp, 67.40.Db, 75.10.Jm

About 2000 years ago, early Chinese chemists synthesized barium copper silicates for the first time, and used them as pigments for pottery and trading as well as for large Empire projects such as the Terracotta Warriors [1, 2, 3], preceding even the invention of paper and the compass.  $\text{BaCuSi}_2\text{O}_6$ , also known as Han Purple [1], is then possibly the first man-made compound containing a metallic bond. In its layered crystallographic structure, pairs of  $\text{Cu}^{2+}$  ions form dimers arranged in a square lattice, with Cu-Cu bonds projected normal to the planes [4]. Neighboring Cu bilayers are weakly coupled, i.e. the magnetic system is quasi-two dimensional [5]. Applied magnetic fields in excess of 23.5T suppress the spin singlet ground state in  $\text{BaCuSi}_2\text{O}_6$ , giving rise to a gas of quantum spin-triplet excitations.

At low temperatures, an ideal gas of bosons undergoes a phase transition into a condensate with macroscopic occupation of the single-particle ground state. A great deal of interest in this phenomenon was triggered by the discovery of the anomalous behavior of liquid helium. Upon cooling, liquid  $^4\text{He}$  exhibits a  $\lambda$ -transition in the specific heat at 2.17 K that signals the onset of a zero-viscosity superfluid state [6]. Superfluidity arises from the macroscopic fraction of He atoms that occupy the single particle ground state. Within the last decade, Bose-Einstein condensation (BEC) was also realized for dilute clouds of atoms at temperatures lower than ten millionths of a degree Kelvin [7]. The possibility of producing BEC with quantum spin magnets[8] has stimulated considerable experimental effort to find the candidate materials[9].

Spin-dimer systems such as  $\text{SrCu}_2(\text{BO}_3)_2$  [10] and  $\text{TiCuCl}_3$  [11] have recently become of interest owing to the ability of strong magnetic fields to generate a gas of  $S^z = 1$  spin-triplet states moving in a non-magnetic background. These *triplons* [17] can be regarded as bosonic particles with hard core repulsions that carry a magnetic moment, but no mass or charge. The external field plays the role of a chemical potential in controlling the number of particles. The Ising component of the inter-dimer exchange interaction generates an effective repulsion between neighboring bosons.

Upon cooling, the gas of triplons can either crystallize or condense in a liquid state, depending on the balance between the kinetic energy and the repulsive interactions [9]. In particular, if the kinetic energy dominates and the number of triplons (or total magnetization) is a conserved quantity, the system undergoes BEC corresponding to the coherent superposition of  $S^z = 1$  spin-triplet and  $S = 0$  singlet states on each and every dimer. The BEC of triplons was proposed to occur in  $\text{TiCuCl}_3$  [11, 12, 13] and  $\text{KCuCl}_3$  [14, 15]. However, recent data suggest that the anisotropic crystal structure of these spin-ladder systems breaks the U(1) rotational invariance that

is required to have gapless Goldstone modes [16]. Hence, the Goldstone modes acquire a finite gap or mass. In this report we introduce a new system whose bi-layer structure provides a realization of a quasi-two dimensional gas of triplons.

The range of fields and temperatures required to obtain a BEC of triplets in  $\text{BaCuSi}_2\text{O}_6$  creates a unique situation from the experimental standpoint: the triplons dominate the thermodynamics in a very simple and predictable fashion. The simplicity of  $\text{BaCuSi}_2\text{O}_6$  is best described by a spin Hamiltonian that includes only the nearest-neighbor Heisenberg antiferromagnetic exchange couplings. The  $\text{Cu}^{2+}$  ions and the  $\text{SiO}_4$  tetrahedra in  $\text{BaCuSi}_2\text{O}_6$  are arranged in layers parallel to the (001) crystallographic plane, as shown in Fig. 1(a). Within each Si-O-Cu layer, the  $\text{Cu}^{2+}$  ions form a square lattice bi-layer of  $S = 1/2$  spins [4]. The relevant Heisenberg exchange couplings within the bi-layers are the intra-dimer interaction,  $J$ , and an inter-dimer nearest-neighbor interaction  $J'$  (Fig. 1(a)). The different bi-layers are antiferromagnetically coupled via the effective exchange constant  $J''$ . The resulting spin Hamiltonian is:

$$H_s = J \sum_{\mathbf{i}} \mathbf{S}_{\mathbf{i},1} \cdot \mathbf{S}_{\mathbf{i},2} + J' \sum_{\mathbf{i},\alpha,\beta} \mathbf{S}_{\mathbf{i},2} \cdot \mathbf{S}_{\mathbf{i}+\hat{e}_\alpha,2} + J'' \sum_{\mathbf{i}} \mathbf{S}_{\mathbf{i},1} \cdot \mathbf{S}_{\mathbf{i}+\hat{z},2} - g_{\parallel} \mu_B H \sum_{\mathbf{i},\beta} S_{\mathbf{i},\beta}^z \quad (1)$$

where  $\alpha = \{1, 2\}$  is the direction index,  $\beta = \{1, 2\}$  is the layer index,  $\hat{e}_1 = \hat{x}$ ,  $\hat{e}_2 = \hat{y}$  and  $\hat{z}$  are unit vectors along the crystallographic axes, and  $g_{\parallel} = 2.306 \pm 0.008$  is the component of the gyromagnetic tensor along the  $c$ -axis, which is the direction of the applied magnetic field  $H$ . The value of  $J = 4.5\text{meV}$  is known from inelastic neutron scattering studies. [5], which also show that  $J'' \ll J' \ll J$ . Precise values of

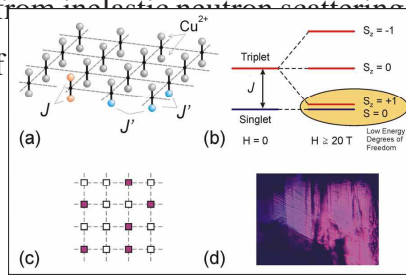


FIG. 1: (color online) a)  $\text{Cu}^{2+}$ -dimer plane in  $\text{BaCuSi}_2\text{O}_6$  in a square lattice arrangement.  $J$  and  $J'$  are the intra-dimer and inter-dimer exchange constants. b) Evolution of the isolated dimer spin singlet and triplet with an applied magnetic field  $H$ . c) Partially occupied hard core boson lattice. Occupation (chemical potential) is given by the external magnetic field. d) Transmission-light picture of a  $\text{BaCuSi}_2\text{O}_6$  single crystal.

In the limit  $J' = J'' = 0$ , the ground state of  $H_s$  is a product of local singlet-dimer states:  $|\Psi_0\rangle = \otimes_i |\phi_i^s\rangle$  where  $|\phi_i^s\rangle$  is the singlet state between two spins on a dimer  $i$ .  $J = 4.5$  meV is the energy gap for a spin triplet excitation in a single isolated dimer [5]. This gap decreases linearly with an applied magnetic field as shown in Figure 1(b). Since  $J'', J' \ll J$ , the spectrum is dominated by the two low energy states of the isolated dimer (the  $S = 0$  singlet and the  $S^z = 1$  triplet) once  $g_{\parallel}\mu_B H$  becomes of the order of  $J$ . By projecting  $H$  onto this low energy subspace, we derive an effective Hamiltonian,  $H_{eff}$ , in which each dimer is represented by one effective site with two possible states. In this way, we are neglecting the effect of the high energy triplet states and, therefore, the highest order terms of  $H_{eff}$  are linear in  $J'$  and  $J'' = 0$  (first order perturbation theory). A similar procedure was used before by Mila [18] to describe spin ladders in a magnetic field. We associate the two low energy states with the two possible states of a hard core boson on a lattice [5] (see Fig. 1(c)). The empty site corresponds to the singlet state  $|\phi_i^s\rangle$ , while the site occupied by the hard core boson represents the  $S^z = 1$  triplet state:  $|\phi_i^s\rangle \rightarrow |0\rangle_i$ ,  $|\phi_i^t, S^z = 1\rangle \rightarrow b_i^\dagger |0\rangle_i$ , where  $|0\rangle_i$  represents the empty state at the site  $i$ . In this language, the effective low energy Hamiltonian is:

$$\begin{aligned}
H_{eff} = & t \sum_{i,\alpha} (b_{i+\hat{e}_\alpha}^\dagger b_i + b_i^\dagger b_{i+\hat{e}_\alpha}) + t' \sum_i (b_{i+\hat{z}}^\dagger b_i + b_i^\dagger b_{i+\hat{z}}) \\
& + V \sum_{i,\alpha} n_i n_{i+\hat{e}_\alpha} + V' \sum_i n_i n_{i+\hat{z}} + \mu \sum_i n_i
\end{aligned} \tag{2}$$

where the chemical potential is  $\mu = J - g_{\parallel}\mu_B H$ ,  $t = V = J'/2$ , and  $t' = V' = J''/4$ . Eq. 2 describes a gas of hard core bosons with nearest-neighbor hopping and repulsive interactions. For  $H$  less than a critical field  $H_{c1}$  ( $g_{\parallel}\mu_B H_{c1} = J - 2J' - J''/2$ ), the ground state of  $H_{eff}$  is completely empty, i.e. all dimers are spin singlets, because the chemical potential,  $\mu$ , is large and positive. A finite concentration of particles  $\rho = m$  ( $m$  is the magnetization per site) emerges in the ground state only when  $H$  exceeds  $H_{c1}$ . Because the condition  $V \leq 2t$  is not fulfilled, the triplets or hard core bosons never crystallize for any concentration  $\rho < 1$ .

The single crystal samples used in this study were prepared using the floating-zone technique.  $\text{BaCO}_3$ ,  $\text{CuO}$ , and  $\text{SiO}_2$  were used as starting materials and the powders of stoichiometric compositions were mixed and sintered at  $700^\circ\text{C}$  for 15h. The sintered powder was reground and molded into a rod under a pressure of  $400\text{kg}/\text{cm}^2$  for about 10min. The rod is sintered between  $1000$  and  $1100^\circ\text{C}$  for about 100 h. The sintered rod is then used for floating zone method [22]. The floating

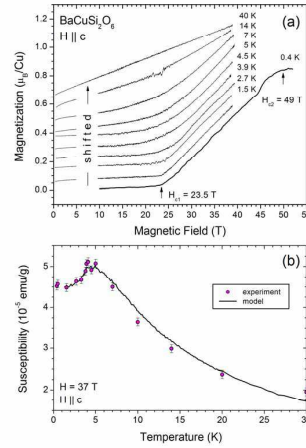
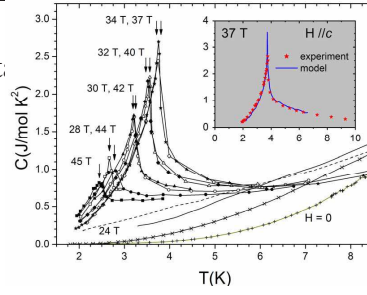


FIG. 2: (color online) a) Magnetization vs field at different temperatures from 0.4 K to 40 K, measured in both a 65 T short-pulse, and a 45 T mid-pulse, capacitor driven pulsed magnets. b): Magnetic susceptibility vs temperature from measurements in A, and from our model using a quantum Monte Carlo algorithm.

zone growth was done twice. In the first run the speed of the growth was set to 50 mm/h, and in the second run to  $\sim 0.5$  mm/h, both in  $O_2$  flow of  $\sim 200$  cc/min. The purple color and texture of our single crystal sample is appreciated in a picture taken in transmission (backlight) mode (Fig. 1(d)). Figure 2a shows the magnetization versus field data obtained in capacitor-driven pulsed magnetic fields [19]. The magnetization increases continuously between the critical field  $H_{c1} = 23.5$  T and the saturation field  $H_{c2} = 49$  T at  $T = 0.4$  K. The nearly linear slope of the magnetization contrasts sharply the staircase of plateaux observed in  $SrCu_2(BO_3)_2$ , where the gas of triplets is known to crystallize in a structure that is commensurate with the underlying crystallographic lattice [9, 10]. Pulsed magnetic field experiments on  $BaCuSi_2O_6$  were repeated at different temperatures up to 40 K and cross-calibrated against low-field SQUID magnetometer data [5]. The structure observed around  $\simeq 48$  T at low temperatures, which we could not reproduce in later experiments, is likely an artifact caused by mechanical vibration of the probe. A plot of the slope  $\chi = dM/dH$  of  $M$  versus  $H$  (magnetic susceptibility) at  $H = 37$  T is shown in figure 2(b) together with the results of a Monte Carlo simulation of  $H_{eff}$  in a finite lattice of size  $L^3$ , with  $L = 12$ , performed using the directed-loop algorithm [20, 21] with parameters:  $J = 4.45$  meV,  $J' = 0.58$  meV and  $J'' = 0.2J' = 0.116$  meV. The agreement between experimental data and model calculations is remarkable. Notably, the rapid drop of the magnetic susceptibility below 4 K indicates the onset

of an ordered low temperature state.



sate.

FIG. 3: (color online) Specific heat vs temperature at constant magnetic fields  $H$ . A low temperature  $\lambda$ -anomaly is evident at  $H \geq 28$  T. The anomaly first moves to higher temperatures with increasing magnetic fields, it reaches a maximum at  $H = 36 \pm 1$  T, and then decreases for  $37 < H < 45$  T. Inset: Specific heat vs  $T$  at  $H = 37$  T after subtraction of a small contribution due to the  $S^z = 0$  triplet level only relevant at higher temperatures, and phonons. Also displayed is the result of our Monte Carlo calculation.

The observation of a phase transition is further confirmed by specific heat measurements as a function of temperature for constant magnetic fields shown in Figure 3. This experiment was performed in a calorimeter made out of plastic materials [23] using both a superconducting magnet and the 45 T hybrid magnet at the National High Magnetic Field Laboratory. At zero magnetic field the specific heat is featureless. As soon as finite external field along the  $c$ -axis is applied the specific heat increases due to the reduction in the singlet-triplet energy gap  $\Delta(H)$ . A small anomaly then develops for  $H = 28$  T at  $T \sim 2.7$  K that moves to higher temperatures as the magnetic field is further increased. This  $\lambda$ -shaped anomaly also grows with magnetic field due to the increased number of triplons (magnetization). Their number at low temperatures is roughly proportional to the magnetic field (see Figure 2(a)). Once the middle of the magnetization ramp is reached at  $H = 36 \pm 1$  T, the transition temperature and the size of the  $\lambda$ -anomaly then start to decrease owing to the reduction in the availability of singlet dimers. Moreover, the mirror symmetry of the phase diagram around this maximal point (see Fig. 4) offers an experimental confirmation of the *particle-hole symmetry* implicit in  $H_{eff}$ . No phonon contribution has been subtracted from the specific heat data. The inset of figure 3 displays the data at 37 T after subtraction of a small exponential contribution (activated energy  $\Delta(H = 0) = 3.13$  meV) from the  $S^z = 0$  triplet components that becomes apparent only above 8 K. In addition, a Debye phonon contribution with  $\Theta_D = 350$  K was subtracted. The solid line is the result of our quantum Monte Carlo calculation for  $H_{eff}$  after a finite size scaling to the thermodynamic limit. The systems sizes that were used for the scaling are:  $L = 4, 6, 8, 12$ .

The phase diagram of figure 4 shows all our experimental data combined, together with some temperature traces measured while sweeping the magnetic field at a rate of about 12 T/min, i.e.

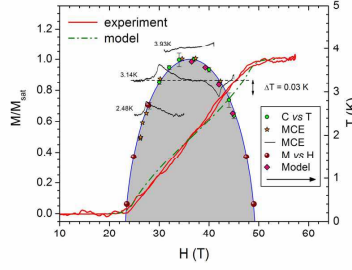


FIG. 4: (color online) Left  $y$ -axis: Magnetization normalized to the saturation value ( $M/M_{sat}$ ) vs magnetic field along the  $c$ -axis, measured at 1.5 K (red line). Results for the model discussed in the text (green line). Right  $y$ -axis: Transition temperature from specific heat vs temperature, magnetocaloric effect (MCE) and magnetization vs field data. Black lines are the sample temperature measured while sweeping the magnetic field quasi-adiabatically.

magneto-caloric effect (MCE) [24]. The left side  $y$ -axis is for the magnetization versus  $H$  curve. From this curve we obtain:  $H_{c1} = 23.5$  T and  $H_{c2} = 49$  T. The right side  $y$ -axis is for the transition temperature versus field plot obtained from the specific curves (see figure 3) and the magneto-caloric effect measurements. The anomalies in the MCE, observed upon crossing the phase boundaries in the direction of increasing fields, evidence reduced magnetic entropy within the critical region consistent with a gas-to-liquid phase transition. Also displayed in figure 4 are the transition points calculated with our Monte Carlo algorithm for  $L = 12$ . The BEC phase is represented by the shaded region whose boundary is intended merely as a guide to the eye. The excellent agreement between experiment and theory is a compelling case for  $\text{BaCuSi}_2\text{O}_6$  being a true realization of a quasi two dimensional BEC of magnetic degrees of freedom.

Early Chinese chemists could not have imagined two thousand years ago that  $\text{BaCuSi}_2\text{O}_6$  was not only an attractive purple pigment but also a potential solid state device for exploring the quantum effects of a BEC at liquid  $^4\text{He}$  temperatures in magnetic fields. Indeed, we show that a minimal Hamiltonian for a lattice gas of hard core bosons describes surprisingly well the magnetization and specific heat of this magnetic system in external magnetic fields. To derive an effective Hamiltonian we simply neglected the high energy triplet states  $|\phi_i^t, S^z = 0\rangle$  and  $|\phi_i^t, S^z = -1\rangle$ . The excellent agreement with the experimental data, and the verification of the particle-hole symmetry implicit in  $H_{eff}$  validate our approach. However, other physical properties such as the small staggered magnetization that appears in the  $ab$  plane, when the triplets condense, would require the inclusion of virtual processes that involve the above mentioned states. It is also important to remark that the phase coherence of the spin BEC requires the conservation of the number of particles that is equivalent to the total magnetization. This condition is fulfilled whenever the crystal has some degree of rotational symmetry about the direction of the applied field like, for instance,



a four-fold symmetry axis. Otherwise, the presence of anisotropy terms will significantly reduce the de-coherence time of the condensate. Finally, the weakly coupled Cu-bilayers in the crystal structure of  $\text{BaCuSi}_2\text{O}_6$  open the door for future studies like the dimensional crossover of a bosonic gas. By increasing the distance between adjacent bilayers with chemical substitutions the  $\lambda$ -shaped second order phase transition, characteristic of a three-dimensional system, is replaced by a Kosterlitz-Thouless phase transition.

We thank E.W. Fitzhugh for references to early work on Ba-Cu silicates, P. Littlewood, D. Pines and A. Abanov for helpful discussions. Experiments performed at the National High Magnetic Field Laboratory were supported by the U.S. National Science Foundation through Cooperative Grant No. DMR9016241, the State of Florida, and the U.S. Department of Energy.

---

[†] Present address: Central Research Laboratory, Hitachi, Ltd., 1-280, Higashi-Koigakubo, Kokubunji-shi, Tokyo 185-8601, Japan.

[††] Present address: RIKEN (The Institute of Physical and Chemical Research), Wako 351-0198, Japan.

- [1] E.W. FitzHugh, L.A. Zycherman, *Studies in Conservation* **37**, 145 (1992).
- [2] H. Berke, *Angew. Chem. Int. Ed.* **41**, 2483 (2002).
- [3] J. Zuo, X. Zhao, R. Wu, G. Du, C. Xu, C. Wang, *J. Raman Spectrosc.* **34**, 121 (2003).
- [4] L.W. Finger, R.M. Hazen, R.J. Hemley, *Am. Mineral.* **74**, 952 (1989).
- [5] Y. Sasago, K. Uchinokura, A. Zheludev, G. Shirane, *Phys. Rev. B* **55**, 8357 (1997).
- [6] F. London, *Nature* **141**, 643 (1938).
- [7] C.J. Pethick, H. Smith, in *Bose-Einstein condensation in diluted gases*, (Cambridge University Press, Cambridge, 2002).
- [8] T. Matsubara and H. Matsuda, *Prog. Theor. Phys.* **16**, 569 (1956) ; Affleck I., *Phys. Rev. B* **43**, 3215 (1991).
- [9] T.M. Rice, *Science* **298**, 760 (2002).
- [10] H. Kageyama et al., *Phys. Rev. Lett.* **82**, 3168 (1999).
- [11] A. Oosawa et al., *J. Phys.: Condens. Matter.* **11**, 265 (1999).
- [12] T. Nikuni, M. Oshikawa, A. Oosawa, H. Tanaka, *Phys. Rev. Lett.* **84**, 5868 (2000).
- [13] Ch. Ruegg et al., *Nature* **423**, 62 (2003).
- [14] N. Cavadini et al., *Phys. Rev. B* **65**, 132415 (2002).



- [15] A. Oosawa et al., *Phys. Rev. B* **66**, 104405 (2002).
- [16] V. N. Glazkov, A.I. Smirnov, H. Tanaka, A. Oosawa, *Phys. Rev. B* **69**, 184410 (2004).
- [17] K.P. Schmidt and G.S. Uhrig, *Phys. Rev. Lett.* **90**, 227204 (2003).
- [18] F. Mila, *Eur. Phys. J. B* **6**, 201 (1998).
- [19] G.S. Boebinger, A. Lacerda, *Jou. Low Temp. Phys.* **133**, 121 (2003).
- [20] O.F. Syljuasen, A.W. Sandvik, *Phys. Rev. E* **66**, 046701 (2002).
- [21] K. Harada, N. Kawashima, *Phys. Rev. E* **66**, 056705 (2002).
- [22] K. Manabe, H. Ishimoto, N. Koide, Y. Sasago, K. Uchinokura, *Phys. Rev. B* **58**, R575 (1998).
- [23] M. Jaime et al., *Nature* **405**, 160 (2000).
- [24] M. Jaime et al., *Phys. Rev. Lett.* **89**, 287201 (2002).